Brain, Behavior, and Immunity 33 (2013) 131–138

Contents lists available at SciVerse ScienceDirect

Brain, Behavior, and Immunity

journal homepage: www.elsevier.com/locate/ybrbi

The neuroinflammation marker translocator protein is not elevated in individuals with mild-to-moderate depression: A [^{11}C]PBR28 PET study

Jonas Hannestad [a,*], Nicole DellaGioia [a], Jean-Dominique Gallezot [b], Keunpoong Lim [b], Nabeel Nabulsi [b], Irina Esterlis [a], Brian Pittman [a], Jae-Yun Lee [c], Kevin C. O'Connor [c], Daniel Pelletier [b,c], Richard E. Carson [b]

[a] Department of Psychiatry, Yale School of Medicine, New Haven, CT, USA
[b] Department of Diagnostic Radiology, Yale School of Medicine, New Haven, CT, USA
[c] Department of Neurology, Program in Human and Translational Immunology, Yale School of Medicine, New Haven, CT, USA

ARTICLE INFO

Article history:
Received 23 February 2013
Received in revised form 26 June 2013
Accepted 30 June 2013
Available online 9 July 2013

Keywords:
Depression
Neuroinflammation
Microglia
Translocator protein 18 kDa
PET

ABSTRACT

Depression is associated with systemic inflammation. In animals, systemic inflammation can induce neuroinflammation and activation of microglia; however, postmortem studies have not convincingly shown that there is neuroinflammation in depression. The purpose of this study was to use positron emission tomography (PET) with [^{11}C]PBR28, which binds to the neuroinflammation marker translocator protein 18 kDa (TSPO), to compare the level of TSPO between individuals with depression and control subjects. Ten individuals who were in an acute episode of major depression and 10 control subjects matched for TSPO genotype and other characteristics had a PET scan with arterial input function to quantify levels of TSPO in brain regions of interest (ROIs). Total volume of distribution (V_T) of [^{11}C]PBR28 was used as a measure of total ligand binding. The primary outcome was the difference in V_T between the two groups; this was assessed using a linear mixed model with group as a between-subject factor and region as a within-subject factor. There was no statistically significant difference in [^{11}C]PBR28 binding (V_T) between the two groups. In fact, 7 of 10 individuals with depression had lower [^{11}C]PBR28 binding in all ROIs compared to their respective genotype-matched control subjects. Future studies are needed to determine whether individuals with mild-to-moderate depression have *lower* TSPO levels and to assess whether individuals with severe depression and/or with elevated levels of systemic inflammation might have *higher* TSPO levels than control subjects.

1. Introduction

Depression is a debilitating disease that has a 1-year prevalence of 4–5% in men and 8–9% in women, and a lifetime prevalence of 16.5% (www.nimh.nih.gov/statistics). The etiology of depression is not well understood; however, genetic factors, exposure to stress, and impairment in neuroplasticity are all believed to play a role (Krishnan and Nestler, 2010; Wager-Smith and Markou, 2011). In addition, a large body of literature suggests that immune mediators may contribute to depression (Wager-Smith and Markou, 2011). For instance, some individuals with depression have increased blood levels of the inflammatory cytokines tumor necrosis factor alpha (TNFα) and interleukin 6 (IL-6) (Dowlati et al., 2010); however, it is not known whether this is a *result* of depression or potentially a contributing *cause*. In animal models, stress can increase systemic inflammation and neuroinflammation, including activation of microglia (Sugama et al., 2009; Hinwood et al., 2012). In individuals with multiple sclerosis, stress was associated with new inflammatory brain lesions as detected by magnetic resonance imaging (MRI), whereas stress management was shown to reduce such lesions (Mohr et al., 2012). Therefore, it is possible that the stress associated with repeated depressive episodes (or the stress that contributes to causing depressive episodes) leads to systemic inflammation, rather than the other way around. Arguing against this notion is the fact that successful treatment of depression with antidepressant medications does not lead, at least in the short term, to normalization of increased levels of inflammatory cytokines, as shown in a meta-analysis (Hannestad et al., 2011a). Moreover, a recent trial suggested that anti-TNFα therapy with infliximab may ameliorate depressive symptoms in patients with levels of high-sensitivity C-reactive protein (hsCRP) >5 mg/L (Raison et al., 2012), an inflammatory marker that is associated with depression (Wium-Andersen et al., 2012). This suggests that systemic inflammation may contribute to producing depressive symptoms. In support of this, a large body of literature shows that inflammatory stimuli can produce depressive-like symptoms in individuals without depression (Wright et al., 2005; Capuron et al., 2007, 2009;

* Corresponding author. Address: UCB Pharma SA, Chemin du Foriest, B-1420 Braine-l'Alleud, Belgium. Tel.: +32 23 86 36 41.
E-mail address: jonas.hannestad@yale.edu (J. Hannestad).

0889-1591/$ - see front matter © 2013 Elsevier Inc. All rights reserved.
http://dx.doi.org/10.1016/j.bbi.2013.06.010

Eisenberger et al., 2010a,b; Hannestad et al., 2011b; Dellagioia et al., 2013) and modulate neuronal activity in regions that are implicated in depression (Capuron et al., 2007; Harrison et al., 2009; Eisenberger et al., 2010a,b; Hannestad et al., 2012b; Inagaki et al., 2012). Although the question of whether inflammation is a cause or an effect of depression has not been resolved, some evidence suggests that inflammation may contribute to specific symptoms in individuals with depressive disorders. This could be mediated by activation of microglia and production of inflammatory mediators in the brain.

Positron emission tomography (PET) imaging of translocator protein (18 kDa) (TSPO) can be used to detect activated microglia in the brain (Venneti et al., 2006; Rupprecht et al., 2010); however, it is important to keep in mind that reactive astrocytes can also express TSPO (Lavisse et al., 2012). Because an increase in binding of a TSPO radiotracer detected by PET can be due to microglial and/or astrocyte activation, we will henceforth refer to an increase in TSPO binding as evidence of neuroinflammation. Expression of TSPO is low in a healthy brain, but is increased in pathologies that are associated with neuroinflammation, including stroke, trauma, infection, and autoimmune and neurodegenerative disorders (Cosenza-Nashat et al., 2009; Batarseh and Papadopoulos, 2010).

We recently showed that systemic endotoxin administration in nonhuman primates caused neuroinflammation that could be measured with PET and [^{11}C]PBR28 (Hannestad et al., 2012a). Whether neuroinflammation occurs in depression has not been adequately addressed. A postmortem study of individuals who committed suicide found increased microglial density (Steiner et al., 2008); however, no published study has addressed this question *in vivo* with PET imaging. Thus, the aim of this study was to compare [^{11}C]PRB28 binding between subjects with depression and matched control subjects. Our primary hypothesis was that binding would be higher in depression.

2. Materials and methods

2.1. Subjects

In this cross-sectional PET imaging study, 12 medically-healthy subjects with depression and 10 healthy control subjects had a [^{11}C]PBR28 PET scan within 3 weeks of screening. All subjects met the following criteria: (1) Age 18–50; (2) Ability to speak and write English and to give voluntary written informed consent; (3) No active medical conditions or treatments; (4) No illicit substance use in the last 3 months; (5) No history of substance dependence. Healthy control subjects had no history of any psychiatric diagnosis. At the time of screening, subjects with depression met criteria for a Major Depressive Episode as defined in the Diagnostic and Statistical Manual of Mental Disorders, 4th Edition, Text Revision (DSM-IV) (APA, 2000) and could have no other psychiatric diagnosis except for co-morbid anxiety disorders. We reassessed the severity of symptoms at the time of the PET scan to determine whether subjects with depression remained in a depressive episode. Individuals who were taking antidepressant medications were allowed to participate if the dose had been stable for at least 4 weeks. Individuals who had stopped taking antidepressants had to have stopped at least 4 weeks before the study. Eligibility was confirmed through comprehensive psychiatric histories and a Structured Clinical Interview for the DSM-IV (SCID-I) (First et al., 1997). The Montgomery–Åsberg Depression Rating Scale (MADRS) and the Beck Depression Inventory (BDI) were used to determine the severity of the current depressive episode. Medical history and lifetime use of psychiatric medications were obtained. A board-certified psychiatrist confirmed the psychiatric diagnosis and medical history, and performed a physical examination. In addition, subjects were evaluated with the following clinical zchemistry and cytology labs: complete blood count and differential, chemistries, liver function tests, thyroid function tests, hemoglobin A1C, and hsCRP. They also had negative serologies for hepatitis A, B, and C, and HIV, a normal EKG, and a negative urine screen for drugs of abuse. Body mass index was recorded and lipid profile measured because adipose tissue produces inflammatory cytokines. Alcohol misuse was ruled out by history, urine alcohol test, serum GGT, and a breathalyzer at screening and on the day of the PET scan. Pregnancy in women was ruled out by a serum beta-HCG test at screening and a urine beta-HCG test before the PET scan.

The study was conducted under a protocol approved by the Yale Human Investigation Committee, the Yale University Radiation Safety Committee, the Yale-New Haven Hospital Radiation Safety Committee, and the Yale Magnetic Resonance Safety Committee. Subjects were recruited from New Haven and surrounding areas by advertisement and referrals. Written informed consent was obtained from all participants following a full explanation of study procedures.

2.2. Genotyping

The PET radiotracer [^{11}C]PBR28 binds to TSPO with high affinity (K_d = 1.8 nM) (Kreisl et al., 2010); however, the rs6971 missense mutation (a C → T transition that results in an Ala147Thr substitution) reduces the affinity of [^{11}C]PBR28 for TSPO. In homozygotes for the minor allele (T/T), the affinity of [^{11}C]PBR28 for TSPO is very low, resulting in minimal binding and no measurable signal from PET imaging. In heterozygotes (C/T) the PET signal is measurable but lower than in homozygotes for the major allele (C/C) (Owen et al., 2012). The existence of this polymorphism was reported after over half of our subjects had been scanned. At that juncture, we chose to genotype all our subjects and to match by genotype. Whole blood was collected in PAXgene® tubes (Qiagen), and genomic DNA was isolated using the PAXgene Blood DNA kit (PreAnalytiX) according to the manufacturer's instructions. The rs6971 polymorphism was genotyped by performing real-time PCR on a StepOnePlus™ real-time PCR system (Applied Biosystems, CA, USA) as previously described (Owen et al., 2012), using the TaqMan® assay for rs6971 (C_2512465_20; part no. 4351379, Life Technologies, CA, USA). A reaction mixture of 20 μL contained 20 ng genomic DNA, 10 μL of 2× TaqMan® Genotyping Master Mix, 1 μL of the primers and probes mixture, and 7 μL of water. The reactions were incubated for 30 s at 60 °C and 10 min at 95 °C, followed by 40 cycles at 92 °C for 15 s and 60 °C for 1 min. After PCR amplification, endpoint plate read and allele calling was performed using the StepOne Plus PCR System and the corresponding software (v2.1). A plasmid harboring the human TSPO gene (GeneCopoeia, MD, USA) was used as a control for the C/C sequence.

2.3. Magnetic resonance imaging

To allow co-registration of PET and magnetic resonance (MR) images for analysis, each subject had an MR scan on a 3T whole-body scanner (Trio, Siemens Medical Systems, Erlangen Germany) with a circularly-polarized head coil. The following magnetization-prepared rapid-acquisition with gradient echo (MPRAGE) sequence was used: sagittal 3D turbo flash; 250 field of view; 1 mm thick slices; 176 slices total; echo time: 2.78; repetition time: 2500; inversion time: 1100; flip angle: 7; 256 × 256 2 averages. The dimension and pixel size of MR images were 256 × 256 × 176 and 0.98 × 0.98 × 1.0 mm^3, respectively.

2.4. Radiotracer synthesis

The precursor and the reference standard for [^{11}C]PBR28 were provided by the NIMH Chemical Synthesis and Drug Supply Program. [^{11}C]PBR28 was labeled with [^{11}C]methyl triflate using the TRACERLab™ FxC automated synthesis module (GE Medical Systems), or with [^{11}C]methyl iodide using the AutoLoop™ (Bioscan Inc., Washington, D.C.) and the TRACERLab™ Fx-MeI for generating the required [^{11}C]methyl iodide. Specific activity, chemical purity, and radiochemical purity of [^{11}C]PBR28 were determined by radio high performance liquid chromatography (HPLC) coupled with a gamma detector. Specific activity was determined by counting an aliquot in a dose calibrator and determining the mass by HPLC against a calibration curve of the cold standard. Identity was confirmed by co-injecting the standard. At the end of synthesis, the average radiochemical yield (based on trapped [^{11}C]methyl iodide or [^{11}C]methyl triflate) was 9.2% ± 3.8% (n = 24) and the specific activity was 220 ± 149 MBq/nmol (5.94 ± 4.02 mCi/nmol). The average chemical and radiochemical purity were 94.8% and 99.8%, respectively.

2.5. PET imaging

A catheter was inserted in the radial artery by an experienced physician. This arterial line remained in place until the end of scanning and was used for rapid blood sampling to obtain the arterial input function. A transmission scan with a ^{137}Cs point source was obtained before each emission scan. Approximately 600 MBq of [^{11}C]PBR28 was injected, and a two-hour emission scan was acquired on the High Resolution Research Tomograph (Siemens/CTI, Knoxville, TN, USA), which has a reconstructed image resolution of ~3 mm. Dynamic images (33 frames over 120 min) were reconstructed with corrections for measured attenuation, normalization, random events, scatter, and dead-time with a list-mode OP-OSEM (ordinary Poisson ordered set expectation maximization) algorithm. Head motion was corrected based on measurements with the Vicra (NDI, Waterloo, Canada) on an event-by-event basis.

2.6. Arterial input function measurement

Both continuous and sequential discrete arterial blood samples were taken. For the first 7 min, blood was withdrawn continuously with a peristaltic pump (4 ml/min), and radioactivity in whole blood was measured with a cross-calibrated radioactivity monitor (PBS-101, Veenstra Instruments, Joure, Netherlands). During this period, the pump was briefly stopped to take samples at 3 and 5 min. Thereafter, sequential discrete blood samples were taken in order to measure the arterial input function at 8, 12, 15, 20, 25, 30, 40, 50, 60, 75, 90, 105 and 120 min after tracer injection. Sample volumes ranged from 2 to 10 mL. Plasma was separated from blood cells by centrifugation (3900g for 5 min at 4 °C). Whole blood and plasma samples were counted in a cross-calibrated well counter (Wizard 1480, Perkin Elmer, Waltham, MA, USA). The plasma time-activity curve (TAC) during the first seven minutes was estimated from the continuous whole blood TAC. The ratio of the whole-blood-over-plasma concentration was calculated for each sample drawn between 3 and 120 min, fitted to a linear function and then extrapolated between 0 and 7 min.

In order to measure tracer metabolism in plasma, six selected plasma samples (3, 8, 15, 30, 60 and 90 min postinjection; 2–10 mL) were mixed with urea and citric acid at a final concentration of 8 M urea, and filtered through with a1.0 μm Whatman 13 mm GD/X syringe filter. The filtrate was then analyzed by reverse-phase HPLC using a column-switching system. Up to 5 mL of filtrate was loaded on the HPLC system (Shimadzu, Kyoto, Japan), and a mobile phase of 1% acetonitrile water was eluted through the self-packed capture column with solid phase extraction C18 sorbent (Strata-X, Phenomenex, Torrance, CA, USA) at a flow rate 2 mL/min. Then the content of the capture column was back-flushed onto a Gemini-NX analytical column (150 × 4.6 mm, 5 μm) (Phenomenex, Torrance, CA, USA), with a mobile phase consisting of 55:45 0.1 M ammonium hydroxide: acetonitrile at a flow rate of ~1.65 mL/min for the analytical column. The output of the HPLC column was connected to a fraction collector (CF-1 Fraction Collector, Spectrum Chromatography, Houston, TX, USA). Fractions were collected every two minutes and counted in a cross-calibrated well counter.

The ratio of the radioactivity concentrations in filtrate and plasma was obtained and fitted to an exponential raise rise to plateau curve $f_F(t) = a - be^{-\alpha t}$. The unchanged fraction in the filtrate from HPLC was fitted to a integrated gamma function f_H:

$$f_H(t) = a\left(1 - b\left(\int_0^{dt} e^{-u}u^{c-1}du \Big/ \int_0^{\infty} e^{-u}u^{c-1}du\right)\right)e^{-\beta t}$$

The unchanged fraction in plasma was then computed as the product of the functions f_F and f_H. Finally, the arterial input function was computed as the production of the plasma radioactivity concentration and the unchanged fraction.

In order to measure the plasma free fraction (f_P) of [^{11}C]PBR28, ~740 kBq of [^{11}C]PBR28 was added (<25 μl/mL) to a blood sample withdrawn before injection to produce a blood standard. After mixing and centrifugation, plasma water was separated from plasma proteins using ultrafiltration tubes (Centrifree UF device number 4104, Millipore, Billerica, MA, USA) and centrifugation (1100g for 20 min; IEC Medilite centrifuge, Thermo Fisher Scientific, Waltham, MA, USA). Plasma and water samples were counted in triplicate and free fraction was estimated as the ratio of the mean concentration in water and plasma.

3. PET image analysis

Regions of interest (ROIs) were defined using an automated anatomical labeling (AAL) template (Tzourio-Mazoyer et al., 2002) in Montreal Neurological Institute (MNI) space (Holmes et al., 1998). For each subject, the summed PET image was co-registered to the T1-weighted 3T high-resolution MR image using a 6-parameter mutual information algorithm (Wells et al., 1996) (FSL-FLIRT, version 3.2, Analysis Group, FMRIB, Oxford, UK), which was subsequently co-registered to the AAL template in MNI space using a non-linear transform with Bioimage Suite (version 2.5, Yale University). To generate each regional time-activity curve (TAC; results expressed as kBq/mL), the mean radioactivity in the ROI was calculated for each frame as a function of time. The following ROIs were delineated on the template image: frontal, temporal, parietal, and occipital cortex, caudate, putamen, thalamus, cerebellum and white matter (centrum semiovale). TACs were fitted using the one- and two tissue compartment model and the multilinear analysis MA1 (Ichise et al., 2002) which is based on Logan graphical analysis (Logan et al., 1990), using the metabolite-corrected arterial plasma curve as input function, and for MA1 a fit starting time (t^*) of 30 min. Volume of distribution (V_T) values were estimated from the model fits for each ROI. In addition, V_T corrected for plasma free fraction (V_T/f_P) was determined.

3.1. Statistical analysis

The primary hypothesis was that [^{11}C]PRB28 binding (V_T) would be higher in subjects with depression than in matched control subjects. Binding of [^{11}C]PBR28 was compared using a linear mixed model with group (depression, control) as a between-subject factor and region (see ROIs) as a within-subject factor. The best-fitting variance–covariance structure was determined by the Bayesian information criterion. The appropriateness of model selection was

further confirmed by residual analysis. Significant ROI and interaction effects were subsequently analyzed with appropriate post hoc tests. Given the small sample we also performed the nonparametric approach for repeated measures data by Brunner (Brunner et al., 2002). Correlations between [^{11}C]PBR28 binding (V_T) and clinical characteristics were assessed with both Spearman's (nonparametric) and Pearson's (parametric) correlations. All data are reported as mean ± standard deviation (S.D.), and all tests were two-sided and conducted using SAS, version 9.3 (Cary, NC).

4. Results

4.1. Demographic and clinical characteristics

Of 21 case subjects who fulfilled eligibility criteria, 9 subjects consented but did not come back for the PET scan, and 12 case subjects had PET scans. Of the 10 case subjects who had analyzable scans (2 scans were not analyzable, see below), the mean MADRS score was 25.6 ± 7.5 at screening and 19.7 ± 6.7 on the scan day (paired t test, $p = .044$). The mean BDI score was 27.0 ± 9.8 at screening and 20.6 ± 9.5 on the scan day (paired t test, $p = .002$). Two case subjects had co-morbid obsessive–compulsive disorder, 2 were taking antidepressant medications (1 was taking citalopram and 1 was taking paroxetine), and 3 smoked. These data are presented in Table 1.

4.2. Genotypes

Twenty-one subjects were genotyped for this study: 14 were C/C, 6 were C/T, and 1 was T/T; the latter (a healthy control subject) was excluded because of her genotype. Of the subjects who had analyzable PET scans, 3 case subjects were C/T, 6 were C/C, and 1 is unknown (no DNA collected), while 3 control subjects were C/T and 7 were C/C (Table 1). This distribution is in agreement with previous reports (Owen et al., 2012). Of the ones who had analyzable PET scans, there was a higher proportion of the C/T genotype among women (5 C/C, 4 C/T) than among men (6 C/C, 1 C/T).

4.3. PET imaging

Twelve case subjects had a PET scan; however, in two female case subjects (1 African-American and 1 Caucasian, ages 25 and 26, respectively) the PET scan could not be reliably analyzed, due to loss of arterial input function in one and excessive head movement in the other. These subjects were therefore excluded from the analysis.

Analyzable PET scans were obtained in 10 case subjects and 10 control subjects. As detailed in Table 1, these subjects were matched for genotype (except for one case subject in whom DNA was not obtained), sex (9 out of 10 pairs), and age and race to the extent possible. In the depression group, the injected dose (mean ± SD) was 611 ± 133 MBq and the injected mass was 0.055 ± 0.032 μg/kg. In the control group the injected dose was 667 ± 98 MBq and the injected mass was 0.069 ± 0.035 μg/kg. [^{11}C]PBR28 was rapidly metabolized in plasma in both groups, with an unchanged fraction of 66 ± 20%, 13 ± 6% and 4.6 ± 2.4% at 8, 30, and 90 min post injection for control subjects and 72 ± 17%, 17 ± 6% and 6.1 ± 2.6% at 8, 30 and 90 min post injection for case subjects. There was no statistically significant difference in unchanged fraction between the two groups at any time point.

Representative PET images from one control and one case subject are shown in Fig. 1A–B. Early images show a typical white/grey matter contrast attributed to the effect of blood flow. Late images show a very uniform distribution of the radioactivity in the brain. Brain and arterial input time-activity curves from the same subjects are shown in Fig 1C–D.

As previously reported (Fujita et al., 2008), in all regions and for all subjects the two-tissue compartment model provided better fits than the one-tissue compartment model. According to the F-test, the residual sum of squares was significantly higher for the one-tissue compartment model than for the two-tissue compartment model: the minimum $F_{2,29}$ statistic (across all regions and subjects) was 102 (which corresponds to a p value of 8.0×10^{-14}). The tissue time-activity curves were also fitted with MA1 (with a fit starting time t^* of 30 min). The V_T values estimated with MA1 and the 2T model correlated tightly: The regression line equation was $y = 1.005x - 0.033$ and Pearson correlation coefficient was $R^2 = 0.978$, where x and y represents the 2T model and MA1 V_T estimates, respectively. Because the standard errors on V_T estimated from the fit results were 20% lower in average for MA1 than for the 2T model, MA1 V_T values were selected to compare the two groups.

Using mixed-models analysis, there was no effect of group on [^{11}C]PBR28 binding (V_T) ($F(1,18) = 1.4$, $p = .25$) and no group*region interaction ($F(1,18) = 1.1$, $p = .4$) despite numerically lower binding

Table 1
Demographic and clinical characteristics of the matched pairs.

Pair		#1	#2	#3	#4	#5	#6	#7	#8	#9	#10	Mean ± SD
Genotype	Case	C/C	C/C	C/C	C/C	C/C	–	C/C	C/T	C/T	C/T	
	Cont.	C/C	C/C	C/C	C/C	C/C	C/C	C/C	C/T	C/T	C/T	
hsCRP (mg/L)	Case	1.5	<0.2	–	2.6	1.0	1.2	0.4	1.0	1.6	0.9	1.3 ± 0.7
	Cont.	–	0.3	0.8	8.7	1.2	0.2	–	–	1.5	0.3	2.1 ± 3.3
Age (years)	Case	45	26	49	48	19	20	41	48	19	55	37 ± 14
	Cont.	40	32	26	48	25	21	48	49	48	55	39 ± 12
Sex	Case	F	M	M	M	F	F	M	M	F	F	
	Cont.	F	M	F	M	F	F	M	M	F	F	
Race	Case	C	C	C	AA	A	C	C	AA	C	C	
	Cont.	C	C	C	AA	A	C	AA	C	C	C	
BMI	Case	25.9	21.0	27.1	26.3	22.9	22.5	28.2	28.2	–	26.1	25.4 ± 2.6
	Cont.	25.4	22.9	35.3	39.1	25.2	21.5	25.7	22.4	24.9	24.8	26.7 ± 5.8
BDI screen	Case	41	17	31	30	41	32	18	19	27	14	
BDI scan	Case	33	6	25	17	35	21	16	9	27	17	
MADRS screen	Case	26	19	31	30	35	32	14	31	15	23	
MADRS scan	Case	27	16	18	5	30	20	18	23	19	21	
Medication	Case	Par.	–	–	–	–	Cit.	–	–	–	–	
Smoking	Case	–	–	–	–	+	–	–	–	–	+	

A = Asian; AA = African-American; BDI = Beck Depression Inventory; BMI = body mass index; C = caucasian; Cit. = citalopram; Cont. = control subjects; Case = case subjects subjects; hsCRP = high sensitivity C-reactive protein; MADRS = Montgomery–Åsberg Depression Rating Scale; Par. = paroxetine. No data denoted by: –.

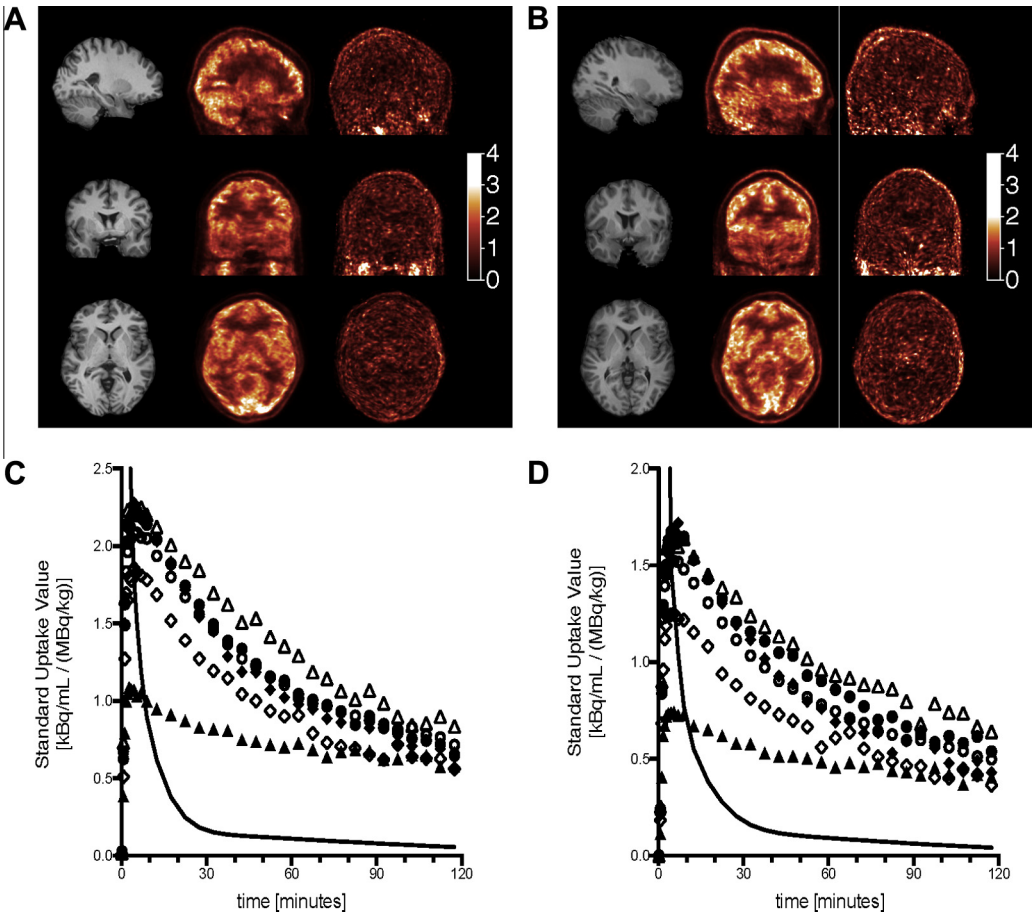

Fig. 1. (A and B) Representative MR (left column) and early PET (0–10 min post injection; center column) and late PET images (90–120 min post injection; right column) from one control subject (A) and one case subject (B) in sagittal (top row), coronal (center row) and axial (bottom row) views. (C and D) Time-activity curves from the same control subject (C) and case subject (D) in selected regions of interest: cerebellum (solid circles), frontal cortex (open circles), caudate (open diamonds), putamen (solid diamonds), thalamus (open triangles) and white matter (solid triangles) and the arterial input function (solid line). The peak of the arterial function is off scale to better display the brain curves.

in all ROIs in the depressed group (Fig. 2). For instance, as illustrated in Fig. 3, in the caudate nucleus 7/10 case subjects had lower binding than their respective matched control subjects. The pattern seen in the caudate was seen in all ROIs. Given the small sample we also performed the nonparametric approach for repeated measures data (Brunner et al., 2002); the nonparametric and parametric results were very similar. Using V_T corrected for plasma free fraction (f_P) instead of V_T did not change these results (data not shown). In the cohort as a whole (depressed and controls), there was a statistically significant difference in mean binding (V_T) between C/C and C/T genotypes in all regions (all $p < .01$), because binding was lower in C/T than in C/C. As can be seen in Fig. 3, the C/T subjects (represented by triangles) have lower binding than all the C/C subjects, except for one.

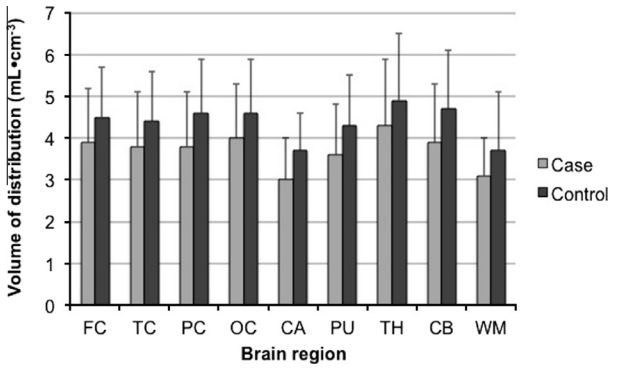

Fig. 2. Mean [^{11}C]PBR28 binding (V_T) in each region in each group. Dark grey bars = control group; light grey bars = case group; FC = frontal cortex; TC = temporal cortex; PC = parietal cortex; OC = occipital cortex; CA = caudate; PU = putamen; TH = thalamus; CB = cerebellum; WM = white matter. Error bars denote standard deviation.

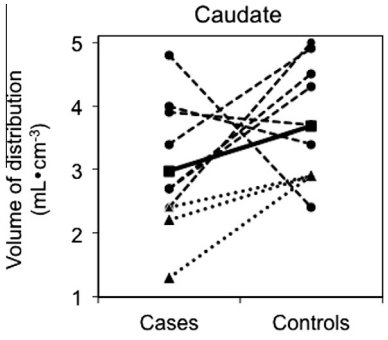

Fig. 3. [^{11}C]PBR28 binding (V_T) in the caudate nucleus for each subject in each group. Circles represent binding for each C/C subject, triangles represent each C/T subject, and the squares represent the mean of all subjects in each group. The dotted lines connect the matched subject pairs (see Table 1 for details on matching). The solid line connects the mean binding levels for the two groups.

4.4. Correlation with clinical characteristics

There was no correlation between [^{11}C]PBR28 binding and age, BMI, or hsCRP in the cohort as a whole or within each group.

Potential differences in binding between men and women could not be assessed due to the different distribution of genotypes among men and women in our cohort. Similarly, potential differences due to race or ethnicity could not be assessed due to the low sample size. There were no correlations between binding and depression severity (MADRS or BDI score). Correlations between binding and antidepressant use could not be assessed because only two subjects were taking antidepressants. Excluding these two subjects and their matched controls from the analysis did not change the results.

5. Discussion

PET imaging with [^{11}C]PBR28 in subjects with mild-to-moderate depression and hsCRP levels <5 mg/L did not show that depressed subjects have neuroinflammation or microglial activation. It is possible that individuals with severe depression and/or a longer history of depression and/or increased systemic inflammation (e.g. hsCRP levels >5 mg/L) could have neuroinflammation. We decided to exclude individuals with elevated hsCRP because such individuals might have an undiagnosed medical condition that is associated with inflammation; our aim was to assess neuroinflammation in subjects with depression who had no indication of any other medical problem so that neuroinflammation, if found, could be attributed to depression.

Interestingly, within the limits of the small sample size, our data suggest that subjects with depression might have *lower* levels of brain TSPO than control subjects. This difference was not statistically significant, but it is important to explore this question further in a larger sample. Anxiety is associated with lower levels of platelet TSPO in healthy individuals (Nudmamud et al., 2000; Nakamura et al., 2002), and lower TSPO binding in platelets has been found in panic disorder, posttraumatic stress disorder, generalized anxiety disorder, and social anxiety disorder (Johnson et al., 1998; Rocca et al., 1998). Lower TSPO binding in platelets has also been found in individuals who attempted suicide (Soreni et al., 1999), but not in depression (Weizman et al., 1995), except when co-morbid with adult separation anxiety disorder (Chelli et al., 2008). Interestingly, TSPO agonists have anxiolytic properties in animal models and in humans (Rupprecht et al., 2010; Costa et al., 2011; Venneti et al., 2013). We did not measure anxiety levels in our cases, but anxiety is often co-morbid with depression and this may be an explanation for the lower levels of TSPO. Nonetheless, it is important to keep in mind that the relationship between brain and platelet TSPO levels is poorly understood.

It is well established that TSPO expression is increased in diseases in which there is neuroinflammation, and that TSPO expression is mostly due to expression in microglia and astrocytes (Cosenza-Nashat et al., 2009). Therefore, an increase in TSPO expression as measured by PET imaging is usually attributed to an increase in the numbers of activated microglia and/or reactive astrocytes. A decrease in TSPO expression is more difficult to explain. Resting microglia are tightly regulated by interactions with neurons (Ponomarev et al., 2011). When provided with signals that indicate tissue damage or infection, microglia become activated, a key event in the initiation and maintenance of neuroinflammation (Chan et al., 2007; Tambuyzer et al., 2009; Chen et al., 2010). Microglia also serve important repair and neuroprotective functions (Hanisch and Kettenmann, 2007; Li et al., 2007), and the phenotype of activated microglia, like that of macrophages, can be on a continuum between two activation "extremes", namely M1 or pro-inflammatory and M2 or anti-inflammatory. Pro-inflammatory stimuli (e.g. LPS) that cause an M1 activation state also cause increased TSPO expression in microglia. What effect activation of microglia with anti-inflammatory stimuli (e.g. interleukin-4 or interleukin-13) has on TSPO expression has not been determined. If M2 microglia also have higher TSPO levels than resting microglia, it is possible that an increase in TSPO expression may indicate either an anti-inflammatory/neuroprotective state *or* a neuroinflammatory/neurotoxic state. If indeed TSPO expression increases in both "good" and "bad" activated microglia, this is a limitation of using TSPO as a microglial marker in brain diseases. Rather than developing improved TSPO PET tracers, efforts should be directed at developing PET tracers that bind to proteins that are expressed on microglia with specific functional phenotypes (i.e. neuroprotective vs. neurotoxic), because such tracers might be more useful in investigating pathophysiology of brain diseases.

We investigated the differences between cases and controls using *a priori* selected regions of interest that were delineated using an anatomical template. Alternative approaches include (1) using automated segmentation in the subject's native MRI space, and (2) voxel-based analyses. We have not tested automated segmentation; [^{11}C]PBR28 is poorly suited to this approach due to its very uniform distribution in the human brain and low white to gray matter contrast. Such a distribution would likely not permit detecting a difference between delineation methods. A potential advantage of computing whole brain parametric images of [^{11}C]PBR28 volumes of distribution and then applying voxel-based statistical analyses, is to avoid the *a priori* selection of region of interest. This might allow the detection of changes in unexpected regions, or changes limited to only a subpart of the selected regions. The main challenge of applying voxel-based analysis is the computation of parametric images of [^{11}C]PBR28 volume of distribution, and in particular the selection of an appropriate noise-filtering method, since full-resolution and unfiltered parametric images of [^{11}C]PBR28 volumes of distribution computed with MA1 are very noisy.

In addition to limitations of TSPO as a marker of neuroinflammation and the limitations of [^{11}C]PBR28 image analysis described above, there are other limitations that should be pointed out. The sample size is small, and given the large inter-subject variability of [^{11}C]PBR28 binding, this makes the study prone to Type I or Type II error; however, in accordance with recent recommendations (Button et al., 2013), we have reported all data exclusions, all data manipulations, and all measures acquired in the study to allow the reader to fully assess and interpret the data. An *a priori* power calculation was not performed because we did not have any data to estimate the possible effect size of the difference in binding. In our sample, the effect size (Cohen's d) ranged from 0.37 in the thalamus to 0.72 in the caudate. If we assume that the current sample is representative of individuals with mild-to-moderate depression with hsCRP levels <5 mg/L, and that these effect sizes are the true effect sizes, we would need 32 subjects in each group to detect a difference in the caudate and 116 subjects in each group to detect a difference in the thalamus (80% power at a two-sided .05 significance level).

Other limitations include the fact that the subjects had mild-to-moderate rather than severe depression and that there was no cut-off with regards to a minimum number of life-time depressive episodes. Lastly, we did not measure TNFα and IL-6 levels in these subjects. The two main strengths of this study are (1) rigorous quantitation of [^{11}C]PBR28 binding with arterial input function and kinetic modeling, and (2) matching for TSPO genotype.

In conclusion, in our cohort of 10 subjects with depression and 10 genotype-matched control subjects we found no statistically significant difference in [^{11}C]PBR28 binding in any of the brain regions assessed. Interestingly, most subjects with depression had lower binding than their respective matched control subject, contrary to our *a priori* hypothesis. Therefore, it is very unlikely that such individuals with depression have higher binding than non-depressed subjects. Further studies are needed to clarify whether

neuroinflammation plays a role in depression and also to determine whether PET imaging of TSPO is a sufficiently sensitive and specific *in vivo* measure of different microglial activity states in brain diseases in general.

Conflict of interest statement

All authors declare that there are no conflicts of interest. Dr. Hannestad became an employee of UCB Pharma after the completion of this study.

Acknowledgments

A Molecular Imaging Research Grant for Junior Medical Faculty from the Society for Nuclear Medicine (J.H.) funded this research. Salary support was provided by K12DA00167 (J.H.). The research was also made possible by infrastructure and nursing support provided by the State of Connecticut, Department of Mental Health and Addiction Services, and by CTSA grant UL1 RR024139 from the National Center for Research Resources (NCRR) and the National Center for Advancing Translational Science (NCATS), components of the National Institutes of Health (NIH), and NIH roadmap for Medical Research. Its contents are solely the responsibility of the authors and do not necessarily represent the official view of NIH. The authors wish to thank the Clinical Neuroscience Research Unit nursing staff, the Yale PET Center staff, Clark Zhang, and the subjects who participated in this study.

References

APA, 2000. Diagnostic and Statistical Manual of Mental Disorders: DSM-IV-TR. American Psychiatric Publisher.

Batarseh, A., Papadopoulos, V., 2010. Regulation of translocator protein 18 kDa (TSPO) expression in health and disease states. Mol. Cell. Endocrinol. 327, 1–12.

Brunner, E., Domhof, S., Langer, F., 2002. Nonparametric Analysis of Longitudinal Data in Factorial Experiments. John Wiley and Sons, New York.

Button, K.S., Ioannidis, J.P., Mokrysz, C., Nosek, B.A., Flint, J., Robinson, E.S., et al., 2013. Power failure: why small sample size undermines the reliability of neuroscience. Nat. Rev. Neurosci. 14, 365–376.

Capuron, L., Fornwalt, F.B., Knight, B.T., Harvey, P.D., Ninan, P.T., Miller, A.H., 2009. Does cytokine-induced depression differ from idiopathic major depression in medically healthy individuals? J. Affect. Disord. 119, 181–185.

Capuron, L., Pagnoni, G., Demetrashvili, M.F., Lawson, D.H., Fornwalt, F.B., Woolwine, B., et al., 2007. Basal ganglia hypermetabolism and symptoms of fatigue during interferon-alpha therapy. Neuropsychopharmacology 32, 2384–2392.

Chan, W.Y., Kohsaka, S., Rezaie, P., 2007. The origin and cell lineage of microglia: new concepts. Brain Res. Rev. 53, 344–354.

Chelli, B., Pini, S., Abelli, M., Cardini, A., Lari, L., Muti, M., et al., 2008. Platelet 18 kDa Translocator Protein density is reduced in depressed patients with adult separation anxiety. Eur. Neuropsychopharmacol. 18, 249–254.

Chen, S.K., Tvrdik, P., Peden, E., Cho, S., Wu, S., Spangrude, G., et al., 2010. Hematopoietic origin of pathological grooming in Hoxb8 mutant mice. Cell 141, 775–785.

Cosenza-Nashat, M., Zhao, M.L., Suh, H.S., Morgan, J., Natividad, R., Morgello, S., et al., 2009. Expression of the translocator protein of 18 kDa by microglia, macrophages and astrocytes based on immunohistochemical localization in abnormal human brain. Neuropathol. Appl. Neurobiol. 35, 306–328.

Costa, B., Da Pozzo, E., Chelli, B., Simola, N., Morelli, M., Luisi, M., et al., 2011. Anxiolytic properties of a 2-phenylindolglyoxylamide TSPO ligand: Stimulation of in vitro neurosteroid production affecting GABAA receptor activity. Psychoneuroendocrinology 36, 463–472.

Dellagioia, N., Devine, L., Pittman, B., Hannestad, J., 2013. Bupropion pre-treatment of endotoxin-induced depressive symptoms. Brain Behav Immun. 31, 197–204.

Dowlati, Y., Herrmann, N., Swardfager, W., Liu, H., Sham, L., Reim, E.K., et al., 2010. A meta-analysis of cytokines in major depression. Biol. Psychiatry 67, 446–457.

Eisenberger, N.I., Berkman, E.T., Inagaki, T.K., Rameson, L.T., Mashal, N.M., Irwin, M.R., 2010a. Inflammation-induced anhedonia: endotoxin reduces ventral striatum responses to reward. Biol. Psychiatry 68, 748–754.

Eisenberger, N.I., Inagaki, T.K., Mashal, N.M., Irwin, M.R., 2010b. Inflammation and social experience: an inflammatory challenge induces feelings of social disconnection in addition to depressed mood. Brain Behav. Immun. 24, 558–563.

First, M.B., Spitzer, R.L., Gibbon, M., Williams, J.B.W., 1997. Structured Clinical Interview for DSM-IV Axis I Disorders – Clinician Version (SCID-CV). American Psychiatric Press, Washington, DC, 1997.

Fujita, M., Imaizumi, M., Zoghbi, S.S., Fujimura, Y., Farris, A.G., Suhara, T., et al., 2008. Kinetic analysis in healthy humans of a novel positron emission tomography radioligand to image the peripheral benzodiazepine receptor, a potential biomarker for inflammation. Neuroimage 40, 43–52.

Hanisch, U.K., Kettenmann, H., 2007. Microglia: active sensor and versatile effector cells in the normal and pathologic brain. Nat. Neurosci. 10, 1387–1394.

Hannestad, J., Dellagioia, N., Bloch, M., 2011a. The Effect of Antidepressant Medication Treatment on Serum Levels of Inflammatory Cytokines: A Meta-Analysis. Neuropsychopharmacology 36, 2452–2459.

Hannestad, J., DellaGioia, N., Ortiz, N., Pittman, B., Bhagwagar, Z., 2011b. Citalopram reduces endotoxin-induced fatigue. Brain Behav. Immun. 25 (2), 256–259.

Hannestad, J., Gallezot, J.D., Schafbauer, T., Lim, K., Kloczynski, T., Morris, E.D., et al., 2012a. Endotoxin-induced systemic inflammation activates microglia: [^{11}C]PBR28 positron emission tomography in nonhuman primates. Neuroimage 63 (1), 232–239.

Hannestad, J., Subramanyam, K., Dellagioia, N., Planeta-Wilson, B., Weinzimmer, D., Pittman, B., et al., 2012b. Glucose Metabolism in the Insula and Cingulate Is Affected by Systemic Inflammation in Humans. J Nucl Med. 53, 601–607.

Harrison, N.A., Brydon, L., Walker, C., Gray, M.A., Steptoe, A., Critchley, H.D., 2009. Inflammation causes mood changes through alterations in subgenual cingulate activity and mesolimbic connectivity. Biol. Psychiatry 66, 407–414.

Hinwood, M., Morandini, J., Day, T.A., Walker, F.R., 2012. Evidence that microglia mediate the neurobiological effects of chronic psychological stress on the medial prefrontal cortex. Cereb. Cortex 22, 1442–1454.

Holmes, C.J., Hoge, R., Collins, L., Woods, R., Toga, A.W., Evans, A.C., 1998. Enhancement of MR images using registration for signal averaging. J. Comput. Assist. Tomogr. 22, 324–333.

Ichise, M., Toyama, H., Innis, R.B., Carson, R.E., 2002. Strategies to improve neuroreceptor parameter estimation by linear regression analysis. J. Cereb. Blood Flow Metab. 22, 1271–1281.

Inagaki, T.K., Muscatell, K.A., Irwin, M.R., Cole, S.W., Eisenberger, N.I., 2012. Inflammation selectively enhances amygdala activity to socially threatening images. Neuroimage 59, 3222–3226.

Johnson, M.R., Marazziti, D., Brawman-Mintzer, O., Emmanuel, N.P., Ware, M.R., Morton, W.A., et al., 1998. Abnormal peripheral benzodiazepine receptor density associated with generalized social phobia. Biol. Psychiatry 43, 306–309.

Kreisl, W.C., Fujita, M., Fujimura, Y., Kimura, N., Jenko, K.J., Kannan, P., et al., 2010. Comparison of [(11)C]-(R)-PK 11195 and [^{11}C]PBR28, two radioligands for translocator protein (18 kDa) in human and monkey: implications for positron emission tomographic imaging of this inflammation biomarker. Neuroimage 49, 2924–2932.

Krishnan, V., Nestler, E.J., 2010. Linking molecules to mood: new insight into the biology of depression. Am. J. Psychiatry 167, 1305–1320.

Lavisse, S., Guillermier, M., Herard, A.S., Petit, F., Delahaye, M., Van Camp, N., et al., 2012. Reactive astrocytes overexpress TSPO and are detected by TSPO positron emission tomography imaging. J. Neurosci. 32, 10809–10818.

Li, L., Lu, J., Tay, S.S., Moochhala, S.M., He, B.P., 2007. The function of microglia, either neuroprotection or neurotoxicity, is determined by the equilibrium among factors released from activated microglia in vitro. Brain Res. 1159, 8–17.

Logan, J., Fowler, J.S., Volkow, N.D., Wolf, A.P., Dewey, S.L., Schlyer, D.J., et al., 1990. Graphical analysis of reversible radioligand binding from time-activity measurements applied to [N-11C-methyl]-(-)-cocaine PET studies in human subjects. J. Cereb. Blood Flow Metab. 10, 740–747.

Mohr, D.C., Lovera, J., Brown, T., Cohen, B., Neylan, T., Henry, R., et al., 2012. A randomized trial of stress management for the prevention of new brain lesions in MS. Neurology 79, 412–419.

Nakamura, K., Fukunishi, I., Nakamoto, Y., Iwahashi, K., Yoshii, M., 2002. Peripheral-type benzodiazepine receptors on platelets are correlated with the degrees of anxiety in normal human subjects. Psychopharmacology (Berl) 162, 301–303.

Nudmamud, S., Siripurkpong, P., Chindaduangratana, C., Harnyuttanakorn, P., Lotrakul, P., Laarbboonsarp, W., et al., 2000. Stress, anxiety and peripheral benzodiazepine receptor mRNA levels in human lymphocytes. Life Sci. 67, 2221–2231.

Owen, D.R., Yeo, A.J., Gunn, R.N., Song, K., Wadsworth, G., Lewis, A., et al., 2012. An 18-kDa translocator protein (TSPO) polymorphism explains differences in binding affinity of the PET radioligand PBR28. J. Cereb. Blood Flow Metab. 32, 1–5.

Ponomarev, E.D., Veremeyko, T., Barteneva, N., Krichevsky, A.M., Weiner, H.L., 2011. MicroRNA-124 promotes microglia quiescence and suppresses EAE by deactivating macrophages via the C/EBP-alpha-PU.1 pathway. Nat. Med. 17, 64–70.

Raison, C.L., Rutherford, R.E., Woolwine, B.J., Shuo, C., Schettler, P., Drake, D.F., et al., 2012. A randomized controlled trial of the tumor necrosis factor antagonist infliximab for treatment-resistant depression: the role of baseline inflammatory biomarkers. Arch. Gen. Psychiatry, 1–11.

Rocca, P., Beoni, A.M., Eva, C., Ferrero, P., Zanalda, E., Ravizza, L., 1998. Peripheral benzodiazepine receptor messenger RNA is decreased in lymphocytes of generalized anxiety disorder patients. Biol. Psychiatry 43, 767–773.

Rupprecht, R., Papadopoulos, V., Rammes, G., Baghai, T.C., Fan, J., Akula, N., et al., 2010. Translocator protein (18 kDa) (TSPO) as a therapeutic target for neurological and psychiatric disorders. Nat. Rev. Drug Discov. 9, 971–988.

Soreni, N., Apter, A., Weizman, A., Don-Tufeled, O., Leschiner, S., Karp, L., et al., 1999. Decreased platelet peripheral-type benzodiazepine receptors in adolescent in patients with repeated suicide attempts. Biol. Psychiatry 46, 484–488.

Steiner, J., Bielau, H., Brisch, R., Danos, P., Ullrich, O., Mawrin, C., et al., 2008. Immunological aspects in the neurobiology of suicide: elevated microglial

density in schizophrenia and depression is associated with suicide. J. Psychiatr. Res. 42, 151–157.
Sugama, S., Takenouchi, T., Fujita, M., Conti, B., Hashimoto, M., 2009. Differential microglial activation between acute stress and lipopolysaccharide treatment. J. Neuroimmunol. 207, 24–31.
Tambuyzer, B.R., Ponsaerts, P., Nouwen, E.J., 2009. Microglia: gatekeepers of central nervous system immunology. J. Leukoc. Biol. 85, 352–370.
Tzourio-Mazoyer, N., Landeau, B., Papathanassiou, D., Crivello, F., Etard, O., Delcroix, N., et al., 2002. Automated anatomical labeling of activations in SPM using a macroscopic anatomical parcellation of the MNI MRI single-subject brain. Neuroimage 15, 273–289.
Venneti, S., Lopresti, B.J., Wiley, C.A., 2006. The peripheral benzodiazepine receptor (Translocator protein 18 kDa) in microglia: from pathology to imaging. Prog. Neurobiol. 80, 308–322.
Venneti, S., Lopresti, B.J., Wiley, C.A., 2013. Molecular imaging of microglia/macrophages in the brain. Glia 61, 10–23.
Wager-Smith, K., Markou, A., 2011. Depression: a repair response to stress-induced neuronal microdamage that can grade into a chronic neuroinflammatory condition? Neurosci. Biobehav. Rev. 35, 742–764.
Weizman, A., Burgin, R., Harel, Y., Karp, L., Gavish, M., 1995. Platelet peripheral-type benzodiazepine receptor in major depression. J. Affect. Disord. 33, 257–261.
Wells 3rd, W.M., Viola, P., Atsumi, H., Nakajima, S., Kikinis, R., 1996. Multi-modal volume registration by maximization of mutual information. Med. Image Anal. 1, 35–51.
Wium-Andersen, M.K., Orsted, D.D., Nielsen, S.F., Nordestgaard, B.G., 2012. Elevated c-reactive protein levels, psychological distress, and depression in 73131 individuals. Arch. Gen. Psychiatry, 1–9.
Wright, C.E., Strike, P.C., Brydon, L., Steptoe, A., 2005. Acute inflammation and negative mood: mediation by cytokine activation. Brain Behav. Immun. 19, 345–350.